Path Controlling of Automated Vehicles for System Optimum on Transportation Networks with Heterogeneous Traffic Stream

Zhibin Chen[a] Xi Lin[b] Yafeng Yin[c*] Meng Li[b]

[a]*Division of Engineering and Computer Science, NYU Shanghai, People's Republic of China*

[b]*Department of Civil Engineering, Tsinghua University, People's Republic of China*

[c]*Department of Civil and Environmental Engineering, University of Michigan, Ann Arbor, United States*

November 10, 2019

Abstract

In the future, when traffic streams comprise a mix of conventional and automated vehicles (AVs), AVs may be employed as mobile actuators to regulate or manage traffic flow across an urban road network to enhance its performance. This paper develops a path-control scheme to achieve the system optimum (SO) of the network by controlling a portion of cooperative AVs (CAVs) as per the SO routing principle. A linear program is formulated to delineate the scheme and determine the minimum control ratio (MCR) of CAVs to achieve SO. The properties of the MCR are mathematically and numerically investigated. Numerical examples based on real-world networks reveal that the SO of most of the tested networks can be achieved with an MCR below 23%. Considering the low market penetration of AVs at early stages of their deployment, we further investigate a joint path-based control and pricing scheme to replicate SO. Numerical examples demonstrate the remarkable synergy of these combined instruments on reducing the MCR with little collected tolling revenue.

Keywords: Automated Vehicle, Mobile Actuator, Path Control, Minimum Control Ratio, System Optimum, Path-Differentiated Pricing

1 Introduction

Automated vehicles (AVs) are expected to offer transformative improvements to existing mobility systems. Although recent developments suggest that the adoption of AV technology is fast-approaching, it will be many years before the adoption is widespread. In the foreseeable future, the traffic stream on road networks will still be heterogeneous, mixed with both conventional vehicles and AVs. It is thus critical to investigate how to leverage AVs in the traffic stream to better manage and operate our road networks. A few studies have been conducted to examine

*Corresponding author. E-mail address: yafeng@umich.edu (Y. Yin).

the feasibility of using AVs as mobile actuators to regulate traffic flow or distribute travel demand across road networks. In particular, regulation can be achieved by either manipulating AVs' travel choices, such as route and departure time choices, or adjusting AVs' driving behaviors, such as speed profiles.

For the former regulation, Zhang and Nie (2018) investigated an optimal-ratio control scheme to control a certain portion of AVs to mitigate the traffic congestion. In their study, the controlled AVs are required to adopt the system optimum (SO) routing principle, while the uncontrolled vehicles still follow the user equilibrium (UE) routing principle to minimize their individual travel times (Wardrop, 1952). For convenience, we refer to them as cooperative AVs (CAVs) and selfish vehicles (SVs), respectively. More specifically, the authors model the optimal-ratio control scheme problem as a bi-level problem, in which the lower level is a mixed equilibrium model (Harker, 1988; Yang et al., 2007; Zhang et al., 2008) considering both CAVs and SVs, and the upper level determines the optimal ratio of these two types of vehicles in a way to minimize the system total cost that includes the total travel cost and control cost. More recently, considering the same routing principles for CAVs and SVs as Zhang and Nie (2018), Li et al. (2018) investigated the stability of a dynamic system and proposed continuous time stability-first and efficiency-first control strategies. The former control strategy aims to stabilize a given disequilibrium at a minimum time, while the latter one minimizes the cumulative system cost over a given transition period. Numerical experiments show that a larger number of CAVs can lower the cumulative system cost, but not necessarily shorten the convergence time. In a parallel effort to this paper, Sharon et al. (2018) presented a linear model to compute the minimal number of CAVs to achieve SO. Their proposed model can be further used to validate whether a given set of CAVs is sufficiently large to achieve SO.

For the latter regulation, utilizing the beyond-line-of-sight motion information collected from neighboring conventional vehicles, Jin et al. (2018) proposed a class of connected cruise control algorithms for AVs to achieve the head-to-tail string stability. Simulation and real-world experiments have been conducted to highlight that the presence of AVs equipped with the proposed control algorithms can improve the safety and energy efficiency of both AVs and conventional vehicles. With the assist of vehicle-to-infrastructure communication technology, Wang (2018) developed an adaptive driving strategy for connected AVs to stabilize downstream speed disturbances of a platoon with non-connected AVs by manipulating the control parameters - e.g., desired time gap and feedback gains - of the connected AVs. Stern et al. (2018) conducted field experiments on a circular track involving 20 conventional vehicles and an AV. Results uncover that the stop-and-go waves can be efficiently dampened by controlling the velocity of the AV. Based on the findings, the authors claimed that it is possible to smooth the traffic flow with less than 5% of AVs. Furthermore, Wu et al. (2018) proposed optimization models to show that, even for typical highway traffic conditions, properly controlling an AV can stabilize a string of up to 16 conventional cars. Based on simulation, Wu et al. (2017) indicated that controlling the accelerations and lane-changing decisions of AVs can stabilize the mixed traffic flow on a multi-lane ring road.

In the same vein, this paper attempts to demonstrate the potential of AVs as control actuators for improving traffic network performance. When combined with another policy or instrument, we show that AVs as control actuators can yield remarkable results. Specifically, we first investigate the control of travelling path of AVs to affect the path choices of conventional vehicles or other uncontrolled AVs in order to achieve SO, i.e, the minimum system travel time. We seek for the the minimum control ratio (MCR) of cooperative AVs or CAVs, and thus call this scheme as a minimum-ratio control scheme (MRCS). In the scheme, CAVs are required to obey the SO

routing principle, similar to Zhang and Nie (2018) and Sharon et al. (2018). The proposed MRCS will be of interest to the traffic management authority, as the obtained MCR can be regarded as the minimum AV penetration rate that the authority should target in order to achieve SO of a road network with mixed traffic stream. Alternatively, it specifies the minimum portion of AVs that the authority should aim to control in a network with high penetration of AVs, given that many AVs will be possessed by private owners or private service providers, who will likely route their AVs in a selfish routing manner (Yang et al., 2008).

The process to calculate the MCR can be naively modeled by the bi-level programming framework. The upper level is for the control center to determine the minimum ratio of CAVs it takes to achieve the minimum total travel time; while the lower level problem is a mixed equilibrium problem involving both CAVs and SVs (conventional vehicles or uncontrolled AVs). Specifically, SVs attempt to minimize their individual travel time when choosing routes while CAVs seek to minimize the system total travel time. However, as the proposed MRCS aims to achieve the minimum total travel time, the aggregate flow distribution resulting from the mixed equilibrium problem must be the SO flow distribution. Given such a property, similar to Sharon et al. (2018), the MRCS problem can be formulated as a linear program, whose global optimal solution can be guaranteed and easily acquired even for large-scale networks. Nevertheless, the MRCS considered in this paper differs from Sharon et al. (2018) in the following two aspects. First, our formulation is path-based, which is more straightforward and easier to follow. Second, in addition to calculating the MCR, we conduct an investigation of the upper bound of the MCR and the key factors affecting MCR, which sheds light on policy making towards the implementation of related AV control schemes.

Moreover, given that the MCR could be high for some networks, and the fact that it will be a long time before the widespread adoption of AV technologies, we combine the proposed path controlling scheme with another market-based instrument, such as congestion pricing and tradable credit (Yang and Wang, 2011), so as to downsize the MCR. The central idea is controlling a portion of CAVs while applying another market-based instrument to manage the route choices of some SVs in a way to jointly achieve SO. While some other schemes also work, this paper selects the path-differentiated pricing scheme proposed by Zangui et al. (2013) for three reasons: 1) the tolling is path based and is thus compatible with the path control of CAVs; 2) path-differentiated pricing can substantially lessen the financial burden on travelers as demonstrated by Zangui et al. (2015); and 3) path differentiation is being enabled by, among others, fast-developing connectivity technologies. We investigate such a path-based control and pricing scheme and formulate it as a bi-objective nonlinear optimization problem aimed to minimize both the control ratio of CAVs and the tolling burden on travelers. The formulation is then linearized and simplified, and solved efficiently by a proposed solution algorithm.

This paper is organized as follows. In the next section, the MRCS problem is formulated as a linear program. The properties of MCR are then mathematically and numerically analyzed in Section 3. In Section 4, based on real-world transportation networks, numerical examples are conducted to unveil their MCRs, and the characteristics of the corresponding MCRs are explored. The joint control and pricing scheme is proposed and tested in Section 5. Section 6 concludes the paper.

For the convenience of readers, Table 1 presents the list of abbreviations used throughout the paper.

Table 1: List of abbreviations

Abbreviate	Description
AV	Automated vehicle
BPR	Bureau of Public Roads
CAV	Cooperative automated vehicle
ETT	Equal-travel-time
FFTT	Free-flow travel time
JCP	Joint control and pricing
JCP-ZR	Joint control and pricing problem with zero revenue
MCR	Minimum control ratio
MMTT	Minimum marginal travel time
MRCS	Minimum-ratio control scheme
OD	Origin-destination
UE	User equilibrium
SO	System optimum
SV	Selfish vehicle
ZCRR	Zero-control-ratio revenue
ZRCR	Zero-revenue control ratio

2 Minimum Ratio Control Scheme

2.1 Modeling framework

Consider a general traffic network $G(N, A)$, where N and A are the sets of nodes and links in the network, respectively. Let W be the set of origin-destination (OD) pairs for the network, and R_w represent the set of paths between OD pair $w \in W$. Let $\bar{d}_w$, d_w^U, and d_w^C, define the total, SV, and CAV travel demands between OD pair $w \in W$, respectively. Further, we use f_r^U and f_r^C to denote the SV and CAV traffic flow on path $r \in R_w$ between OD pair $w \in W$, respectively. Similarly, we use v_a^U and v_a^C to define the SV and CAV traffic flow of link $a \in A$, respectively. Define $t_a(v_a)$ as the travel time function of link $a \in A$, where $v_a = v_a^U + v_a^C$ is the aggregate flow on link $a \in A$, and we assume $t_a(v_a)$ to be a convex and strictly increasing function. Accordingly, the SO flow distribution can be uniquely determined by solving the SO assignment problem, and we denote it as $\bar{\boldsymbol{v}}$. Let $\hat{R}_w \subseteq R_w$ and $\bar{R}_w \subseteq R_w$ denote the sets of shortest paths and the paths with the minimum marginal travel time (MMTT) between OD pair $w \in W$ under the SO flow distribution $\bar{\boldsymbol{v}}$, respectively. Apparently, these two sets are not necessarily mutually exclusive. However, if they are, i.e., $\hat{R}_w \cap \bar{R}_w = \emptyset$, then $MCR = 1$, as all the flows on the shortest paths have to be controlled to switch to adopt the MMTT paths at this scenario. If $\bar{R}_w \subseteq \hat{R}_w$, then $MCR = 0$, as it implies UE is the same as SO.

Given the above setting, the MRCS can be mathematically formulated as the following problem, dubbed as CP:

$$\min_{\boldsymbol{f}^U, \boldsymbol{f}^C, \boldsymbol{d}^U, \boldsymbol{d}^C, \boldsymbol{v}^U, \boldsymbol{v}^C} \sum_{w \in W} d_w^C$$

$$\text{s.t.} \quad v_a^U = \sum_{w \in W} \sum_{r \in \hat{R}_w} f_r^U \delta_{a,r} \qquad \forall a \in A \tag{1}$$

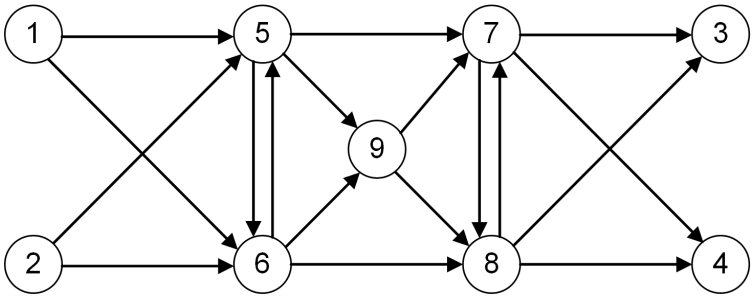

Figure 1: Nine Node network

$$\sum_{r \in \hat{R}_w} f_r^U = d_w^U \qquad \forall w \in W \tag{2}$$

$$f_r^U \geq 0 \qquad \forall r \in \hat{R}_w, w \in W \tag{3}$$

$$v_a^C = \sum_{w \in W} \sum_{r \in \bar{R}_w} f_r^C \delta_{a,r} \qquad \forall a \in A \tag{4}$$

$$\sum_{r \in \bar{R}_w} f_r^C = d_w^C \qquad \forall w \in W \tag{5}$$

$$f_r^C \geq 0 \qquad \forall r \in \bar{R}_w, w \in W \tag{6}$$

$$v_a^U + v_a^C = \bar{v}_a \qquad \forall a \in A \tag{7}$$

$$d_w^U + d_w^C = \bar{d}_w \qquad \forall w \in W \tag{8}$$

In the above problem, constraints (1)-(3) ensure that all SVs will only utilize the shortest paths. It implies that SVs aim to minimize their individual travel time. Constraints (4)-(6) guarantee that the flow of CAVs will only be assigned to the MMTT paths. In other words, the CAVs seek to minimize the system travel time. Moreover, constraint (7) indicates that CAVs are guided to replicate the SO flow distribution (i.e., $\bar{v}$). Taking into account the flow distribution of CAVs and SVs delineated by constraints (1)-(7), the objective function is to minimize the number of CAVs or the MCR, by optimally splitting the total travel demand for each OD pair (see constraint (8)). Note that, in the CP problem, we adopt the path-based formulation rather than its link-based counterpart. With the latter, special treatment is needed to avoid the cyclic flows (Sharon et al., 2018).

As the SO flow distribution (i.e., $\bar{v}$) is predetermined, the shortest path set (i.e., $\hat{R}_w$) and the MMTT path set (i.e., $\bar{R}_w$) for each OD pair can be efficiently enumerated even for large-scale networks (see, e.g., Zangui et al. (2015)). Given $\hat{R}_w$ and $\bar{R}_w$, commercial solvers, such as CPLEX, can be directly applied to solve the CP problem. Another column-generation-based solution algorithm is presented in Appendix A, which does not require such a path enumeration. It is worth highlighting that, the optimal solution regarding the MCR or the minimum number of CAVs (i.e., $\sum_{w \in W} d_w^C$) is unique, but the number of CAVs for each OD pair (i.e., d_w^C) may not be unique. For example, for the Nine Node network in Hearn and Ramana (1998) (see Fig. 1), the MCR is calculated to be 78.70%, while both {10, 20, 8.697, 40} and {10, 20, 20.043, 28.654} are the corresponding CAV demands for OD pair 1-3, 1-4, 2-3, and 2-4.

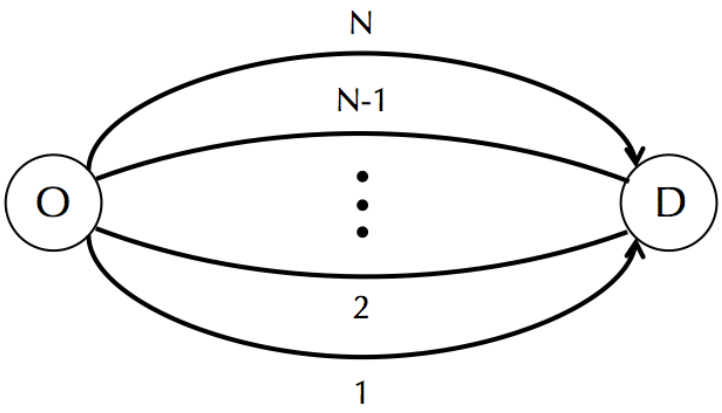

Figure 2: A parallel network

3 Properties of MCR

In this section, we explore the properties of MCR for different types of networks.

3.1 Case of parallel network

In this subsection, we consider a single-OD parallel network shown in Figure 2. Specifically, the OD pair is connected by N parallel links, and the corresponding travel demand is denoted by d. The link travel time function for link $a \in \{1, 2, \ldots, N\}$ is of Bureau of Public Roads (BPR) type form, i.e., $t_a(v_a) = t_a^0 \left[1 + \alpha \left(\frac{v_a}{c_a}\right)^\beta\right]$, where $\alpha > 0, \beta \geq 1$, and t_a^0 and c_a are the free-flow travel time (FFTT) and the capacity of link a, respectively. Without loss of generality, we assume $t_1^0 < t_2^0 \leq \cdots \leq t_N^0$; the first inequality is assumed to be strict because if $t_1^0 = t_2^0 = ... = t_L^0$ for some $L \leq N$, we can equivalently treat them as one link with free-flow travel time t_1^0 and capacity $\sum_{i=1}^{L} c_i$.

Denote the MCR by λ, and the corresponding number of CAVs by d^C, then we have the following proposition.

Proposition 1. $\lambda \leq 1 - \frac{c_1}{\bar{c}N}$, *where* $\bar{c} = \max_{1 \leq a \leq N} c_a$.

Proof. Consider the case where $M(\leq N)$ links are utilized under SO. Denote $g_{\alpha,\beta}(v; c) = 1 + \alpha \left(\frac{v}{c}\right)^\beta$, then by the definition of SO, we have:

$$t_a^0 \left[g_{\alpha,\beta}(v_a; c_a) + v_a \frac{\partial g_{\alpha,\beta}(v_a; c_a)}{\partial v_a}\right] = T \qquad \forall 1 \leq a \leq M \tag{9}$$

where T is a positive number. Here we note that at SO, if there are $M(\leq N)$ links with positive flow, we can easily prove that they are link 1 to link M, i.e., the M links with relatively small values of t_a^0. Eq. (9) can be equivalently written as:

$$t_a^0\left[1+\alpha(1+\beta)\left(\frac{v_a}{c_a}\right)^\beta\right]=T \qquad \forall 1\le a\le M \tag{10}$$

By our setting that $t_a^0 \le t_b^0, \forall 1 \le a < b \le M$, we know $1+\alpha(1+\beta)\left(\frac{v_a}{c_a}\right)^\beta \ge 1+\alpha(1+\beta)\left(\frac{v_b}{c_b}\right)^\beta$, thus $\frac{v_a}{c_a} \ge \frac{v_b}{c_b}$. Hence, we obtain the following inequalities:

$$\frac{t_a^0}{t_b^0}=\frac{1+\alpha(1+\beta)\left(\frac{v_b}{c_b}\right)^\beta}{1+\alpha(1+\beta)\left(\frac{v_a}{c_a}\right)^\beta}\le\frac{1+\alpha\left(\frac{v_b}{c_b}\right)^\beta}{1+\alpha\left(\frac{v_a}{c_a}\right)^\beta}=\frac{g_{\alpha,\beta}(v_b;c_b)}{g_{\alpha,\beta}(v_a;c_a)} \tag{11}$$

Therefore, $t_a^0 g_{\alpha,\beta}(v_a;c_a) \le t_b^0 g_{\alpha,\beta}(v_b;c_b)$, i.e., $t_a(v_a) \le t_b(v_b), \forall 1 \le a < b \le M$. In particular, as $t_1^0 < t_2^0$, we have $t_1(v_1) < t_2(v_2)$. This result suggests that, under SO, only those vehicles on link 1 are guaranteed to be control-free. Combining the result with the fact that $\frac{v_1}{c_1} \ge \frac{v_2}{c_2} \ge \cdots \ge \frac{v_M}{c_M}$, we know:

$$\lambda=1-\frac{v_1}{\sum_{a=1}^M v_a}\le 1-\frac{\sum_{a=1}^M \frac{c_1}{c_a}v_a}{M\sum_{a=1}^M v_a}\le 1-\frac{\frac{c_1}{\bar{c}}\sum_{a=1}^M v_a}{M\sum_{a=1}^M v_a}\le 1-\frac{c_1}{\bar{c}M}\le 1-\frac{c_1}{\bar{c}N} \tag{12}$$

Proof completes. □

Implication of Proposition 1:

a) The MCR (i.e., λ) can be very small when $\frac{c_1}{\bar{c}}$ is large, which may happen when an arterial or highway with high capacity connects two major locations.

b) Building more parallel links to the network, i.e., larger N, may yield higher upper bound for the MCR.

Proposition 2. *λ is nondecreasing with d.*

Proof. We first show that, when there are two scenarios with different demand levels $d_1 < d_2$, and under both cases the SO states are with $M(\le N)$ used links, then $\lambda_1 = \frac{d_1^C}{d_1} \le \lambda_2 = \frac{d_2^C}{d_2}$. The result holds immediately when $M = 1$, so we only consider the case when $M \ge 2$. By Eq. (11), we define:

$$u_a=\frac{t_1^0}{t_a^0}=\frac{1+\alpha(1+\beta)\left(\frac{v_a}{c_a}\right)^\beta}{1+\alpha(1+\beta)\left(\frac{v_1}{c_1}\right)^\beta}\le 1, \forall a\in\{2,3,\dots,M\} \tag{13}$$

Eq. (13) can be rewritten as below:

$$v_a=c_a\left[u_a\left(\frac{v_1}{c_1}\right)^\beta-\frac{1-u_a}{\alpha(1+\beta)}\right]^{\frac{1}{\beta}} \tag{14}$$

With the demand conservation condition, we obtain the following equation:

$$v_1 + \sum_{a=2}^{M} c_a \left[u_a \left(\frac{v_1}{c_1} \right)^{\beta} - \frac{1-u_a}{\alpha(1+\beta)} \right]^{\frac{1}{\beta}} = d \tag{15}$$

Denote $\zeta = \frac{v_1}{d}$, Eq. (15) is then converted to:

$$\zeta + \sum_{a=2}^{M} c_a \left[\frac{u_a}{c_1^{\beta}} \zeta^{\beta} - \frac{1-u_a}{\alpha(1+\beta)d^{\beta}} \right]^{\frac{1}{\beta}} = 1 \tag{16}$$

Denote $J(\zeta, d) = \zeta + \sum_{a=2}^{M} c_a \left[\frac{u_a}{c_1^{\beta}} \zeta^{\beta} - \frac{1-u_a}{\alpha(1+\beta)d^{\beta}} \right]^{\frac{1}{\beta}}$, then we compute the partial derivative by $\frac{\partial J(\zeta,d)}{\partial \zeta} = 1 + \frac{u_a}{c_1^{\beta}} \zeta^{\beta-1} \sum_{a=2}^{M} c_a \left[\frac{u_a}{c_1^{\beta}} \zeta^{\beta} - \frac{1-u_a}{\alpha(1+\beta)d^{\beta}} \right]^{-\frac{\beta-1}{\beta}} > 0$, $\frac{\partial J(\zeta,d)}{\partial d} = \frac{1-u_a}{\alpha(1+\beta)} \sum_{a=2}^{M} c_a$ $\left[\frac{u_a}{c_1^{\beta}} \zeta^{\beta} - \frac{1-u_a}{\alpha(1+\beta)d^{\beta}} \right]^{-\frac{\beta-1}{\beta}} d^{-\beta-1} > 0$, so by the implicit function theorem, we have:

$$\frac{\partial \zeta}{\partial d} = -\left(\frac{\partial J(\zeta,d)}{\partial \zeta} \right)^{-1} \frac{\partial J(\zeta,d)}{\partial d} < 0$$

which means v_1 varies in a decreasing way with d. Thus we prove our first statement: $\frac{d_1^C}{d_1} = 1 - \frac{v_1}{d_1} \leq 1 - \frac{\tilde{v}_1}{d_2} = \frac{d_2^C}{d_2}$. Under both cases the SO states are with $M(\leq N)$ used links, where $\tilde{v}_1$ is the flow on link 1 when the demand is d_2.

Next we show that, when there are two scenarios with different demand levels $d_1 < d_2$, under each case the SO states are with M_1 and M_2 used links respectively; it is straightforward that $M_1 < M_2$. To prove $\frac{d_1^C}{d_1} \leq \frac{d_2^C}{d_2}$, we consider a series of $d_{M_1+1}, d_{M_1+2}, \ldots, d_{M_2-1}, d_{M_2}$, where d_S is the demand level satisfying that:

Under the associated SO state, $t_S^0 \left[g_{\alpha,\beta}(v_S; c_S) + v_S \frac{g_{\alpha,\beta}(v_S;c_S)}{\partial v_s} \right] = t_a^0 \left[g_{\alpha,\beta}(v_a; c_a) + v_a \frac{g_{\alpha,\beta}(v_a;c_a)}{\partial v_a} \right]$, $\forall a < S$ and $v_S = 0$.

In other words, when demand is d_S, there will be S used links in the SO state, but the flow on link S is zero; it is a "middle state" between those with $S-1$ used links and S used links. With the above result, we have the following inequality:

$$\frac{d_1^C}{d_1} \leq \frac{d_{M_1+1}^C}{d_{M_1+1}} \leq \frac{d_{M_1+2}^C}{d_{M_1+2}} \leq \cdots \leq \frac{d_{M_2}^C}{d_{M_2}} \leq \frac{d_2^C}{d_2}$$

Thus Proposition 2 is proved completely. □

Implication of Proposition 2: The increasing demand magnitude, i.e., larger d, can yield non-decreasing MCR on parallel networks. In other words, under such a network topology, the MCR will increase as traffic congestion becomes more severe.

3.2 Case of equal-travel-time network

In this subsection, we derive properties of MCR for a special set of networks, which we call "equal-travel-time" (ETT) networks. The exact definition of ETT networks is given below.

Definition 1. *A road network is called an equal-travel-time network if the following two conditions are met:*

i) All paths between the same OD pair share the same FFTT.

ii) For travel time function of each link, the flow-dependent component is homogeneous of the same degree, i.e., $t_a(v_a) = t_a^0 + \tau_a v_a^k, \tau_a > 0, k > 0$.

For ETT networks, we have the following proposition.

Proposition 3. $\lambda = 0$ *for ETT networks.*

Proof. We show at EET networks the SO state is exactly the UE state. In SO, for any two paths r_1, r_2 between OD pair $w \in W$ with positive path flows, we have:

$$\sum_{a \in A} \delta_{ar_1}[t_a^0 + (1+k)\tau_a v_a^k] = \sum_{a \in A} \delta_{ar_2}[t_a^0 + (1+k)\tau_a v_a^k] \tag{17}$$

Note that the definition of ETT network indicates that:

$$\sum_{a \in A} \delta_{ar_1} t_a^0 = \sum_{a \in A} \delta_{ar_2} t_a^0 \tag{18}$$

We denote $T_w^0 = \sum_{a \in A} \delta_{ar_1} t_a^0$. Subtracting Eq. (18) from Eq. (17) we obtain:

$$\sum_{a \in A} \delta_{ar_1} \tau_a v_a^k = \sum_{a \in A} \delta_{ar_2} \tau_a v_a^k \tag{19}$$

By adding Eq.(19) with T_w^0, we obtain:

$$\sum_{a \in A} \delta_{ar_1}(t_a^0 + \tau_a v_a^k) = \sum_{a \in A} \delta_{ar_2}(t_a^0 + \tau_a v_a^k) \tag{20}$$

Eq. (20) suggests the travel times on paths r_1 and r_2 are identical. On the other hand, for paths r_1 and r_2 in R_w such that $f_{r_1} > 0$ and $f_{r_2} = 0$, by the property of SO state we have:

$$\sum_{a \in A} \delta_{ar_1}[t_a^0 + (1+k)\tau_a v_a^k] \leq \sum_{a \in A} \delta_{ar_2}[t_a^0 + (1+k)\tau_a v_a^k] \tag{21}$$

By the fact that $\sum_{a \in A} \delta_{ar} t_a^0 = T_w^0, \forall r \in R_w$, we know that:

$$\sum_{a\in A}\delta_{ar_1}\tau_a v_a^k \le \sum_{a\in A}\delta_{ar_2}\tau_a v_a^k \tag{22}$$

Again we add it by T_w^0 to acquire:

$$\sum_{a\in A}\delta_{ar_1}(t_a^0+\tau_a v_a^k) \le \sum_{a\in A}\delta_{ar_2}(t_a^0+\tau_a v_a^k) \tag{23}$$

Now, denoting $\mu_w = \sum_{a\in A}\delta_{ar_1}(t_a^0+\tau_a v_a^k)$, combining Eqs. (20) and (23), we conclude that:

$$\sum_{a\in A}\delta_{ar}(t_a^0+\tau_a v_a^k) = \mu_w \qquad f_r > 0, \forall r \in R_w, w \in W$$
$$\sum_{a\in A}\delta_{ar}(t_a^0+\tau_a v_a^k) \ge \mu_w \qquad f_r = 0, \forall r \in R_w, w \in W$$

This is exactly the UE condition. Therefore, the SO state is the same as the UE state in the ETT networks that we consider. Proof completes. □

One example of ETT network is the one-way grid network shown in Figure 3, in which there are $M \times N$ grids. We assume that the flow-dependent components of all link performance functions are homogeneous of the same degree, and horizontal links on the same column are with the same FFTT, as are vertical links on the same row, while the capacities for different links can be different. With this setting, it is straightforward to derive that for any OD pair in the one-way grid network, the FFTTs for associated paths are identical, and by Proposition 3, the one-way grid network exhibits a MCR of zero.

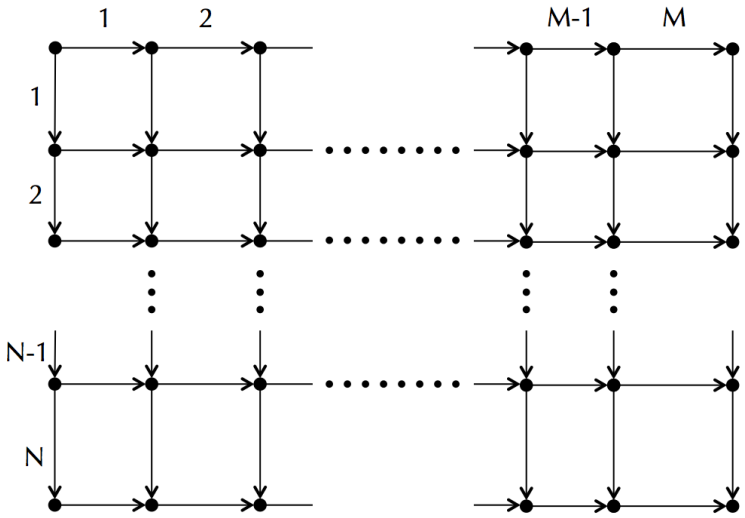

Figure 3: A one-way grid network

The following observation can further relax the condition of the ETT network for achieving SO without any control. Consider an ETT network with an additional path r' between OD pair

$w \in W$ with different FFTT from other paths between the same OD pair, and its FFTT is large enough such that:

$$\sum_{a \in A} \delta_{ar'} t_a^0 > \sum_{a \in A} \delta_{ar} (t_a^0 + \tau_a v_a^k) \qquad \forall r \in R_w, r \neq r'$$

namely, the FFTT of path r' is larger than UE/SO travel time for this OD pair in the original ETT network. Then naturally, at UE there will be no flow on path r', and the modified network is equivalent to the original ETT one. This observation suggests that, if a network is composed of an ETT subnetwork and a set of paths with very large detours, we can still achieve SO without controlling any vehicle; this may apply to a two-way grid network for relatively low demand cases. We must point out that the above conclusion is demand-related; in other words, if the demand is sufficiently large such that the above inequality does not hold anymore, we cannot guarantee UE to be the same as SO

It is worth noting that in certain circumstances, UE can approximate SO with high precision (Colini-Baldeschi et al., 2017; Colini-Baldeschi et al., 2019), but this does not necessarily imply a near-zero or small MCR. For example, consider a parallel network with two links with identical flow-dependent component in the link travel time functions, but with a slight difference in FFTT. In this case, the two links will bear similar amount of traffic in both UE and SO, implying that UE is approximately the same as SO; however, the MCR is around 50% because the flow on at least one link would be under control in achieving SO.

3.3 Case of general network

For general networks, we provide some numerical analyses to illustrate the following properties of MCR. Particularly,

Observation 1. *Increasing demand magnitude may not necessarily yield higher MCR.*

Observation 2. *The demand pattern may have a significant impact on the MCR.*

Observation 3. *All vehicles may need to be controlled to achieve SO.*

Observation 4. *A change in the network topology may have a profound effect on the MCR.*

The evidence of Observation 2 can be found in Section 4.1. Below We demonstrate Observations 1, 3, and 4 by an illustrative example based on the Braess network whose topology is shown in Fig. 4, consisting of one OD pair 1-2 with demand $d(> 0)$. Particularly, linear travel time performance functions are adopted as follows:

$$t_{13} = 10v_{13}$$
$$t_{14} = 50 + v_{14}$$
$$t_{32} = 50 + v_{32}$$
$$t_{34} = 10 + v_{34}$$
$$t_{42} = 10v_{42}$$

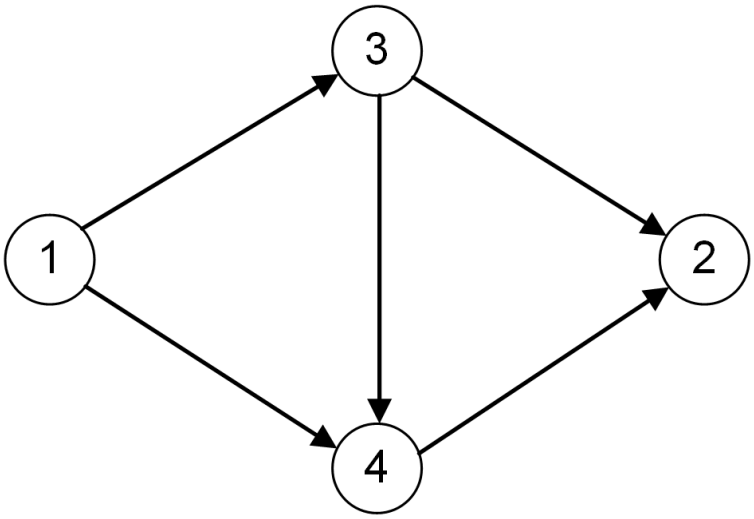

Figure 4: Braess Network

Let f_{132}, f_{142}, and f_{1342} represent the path flows along paths $1 \to 3 \to 2$, $1 \to 4 \to 2$, and $1 \to 3 \to 4 \to 2$. It is easy to verify that the corresponding unique SO flow distribution is given by Table 2. Fig. 5(a) further specifies the path flows along the shortest paths, and Fig. 5(b) presents the calculated MCRs corresponding to different demand magnitudes. As we can see, when $d \leq \frac{80}{9}$, the increase of d yields non-decreasing MCR, which is consistent with Proposition 1. However, when d becomes greater than $\frac{80}{9}$, the MCR drops from 1 to 0. That is because when d changes from $\frac{80}{9}$ to $\frac{80}{9} + \epsilon$ (ϵ is a sufficiently small positive number), paths $1 \to 3 \to 2$ and $1 \to 4 \to 2$ prove to be the shortest paths (see Fig. 5(a)). Therefore, all the flows along these two paths (i.e., $f_{132} + f_{142}$) can be SVs, and the MCR becomes 0. In other words, it is the change of the shortest path set that leads to the considerable decrease in MCR. If we compare the above observation with the proof of Proposition 2, we will see that in the latter, the shortest path set always consists of link 1 (in Fig. 2) no matter how the demand magnitude varies. Accordingly, it may imply that Proposition 2 will hold for general networks if their corresponding shortest path set can remain unchanged when the demand magnitude changes.

In addition, from Fig. 5(b), when $d \in \left[\frac{40}{9}, \frac{80}{9}\right]$, all the vehicles must be controlled (i.e., $\lambda = 1$) in order to achieve SO. Therefore, Observations 1 and 3 have been supported.

In order to highlight Observation 4, we consider the revised Braess networks by removing link $1 \to 4$, $3 \to 2$, or $3 \to 4$ individually. Fig. 6 displays their corresponding MCRs. Compared with Fig. 5(b), it can be found that even with the same demand magnitude, the MCRs will change as the network topology changes. Nevertheless, the changing pattern seems ambiguous. For example, comparing Fig. 6(a) with Fig. 5(b), we can see that removing a link (link $1 \to 4$ or $3 \to 2$) from the original network may yield lower MCR when $d \in \left(\frac{20}{11}, \frac{80}{9}\right]$, but higher MCR when $d \in \left(\frac{80}{9}, +\infty\right]$. However, the comparison between Fig. 6(b) and Fig. 5(b) suggests that removing a link (link $3 \to 4$) from the original network may yield non-increasing MCR under whatever demand magnitude.

Table 2: SO flow distribution

d	f_{132} & f_{142}	f_{1342}
$\left(0, \frac{20}{11}\right]$	0	d
$\left(\frac{20}{11}, \frac{40}{9}\right]$	$\frac{11d-20}{13}$	$\frac{40-9d}{13}$
$\left(\frac{40}{9}, +\infty\right]$	$\frac{d}{2}$	0

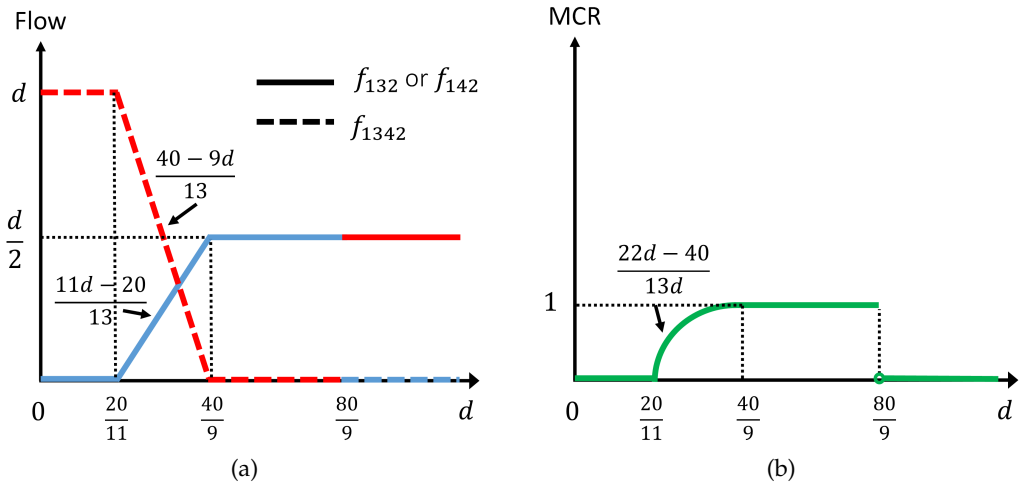

Figure 5: (a) Flow distributions (the red color indicates the path flows on the shortest paths, while the blue color indicates flows on non-shortest paths); and (b) MCRs corresponding to different demand magnitudes

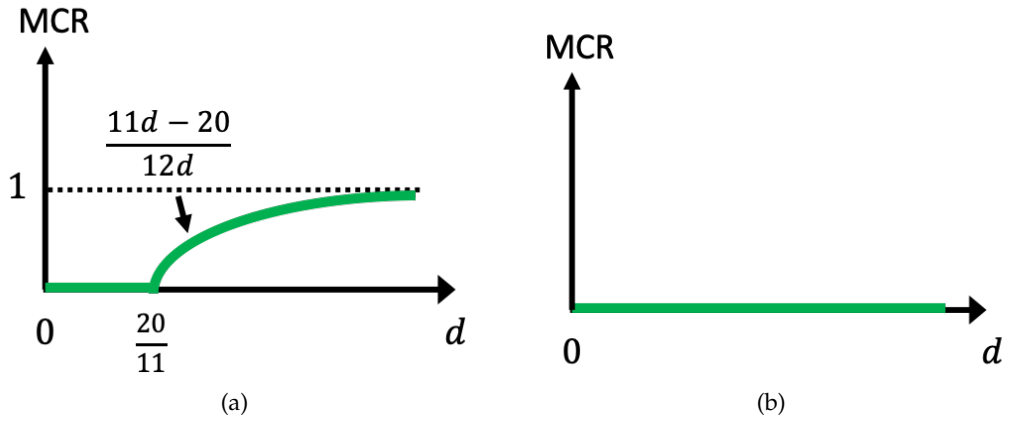

Figure 6: (a) MCRs corresponding to the revised Braess network without link $1 \rightarrow 4$ or $3 \rightarrow 2$; and (b) MCRs corresponding to the revised Braess network without link $3 \rightarrow 4$

4 Numerical Example

In this section, the proposed frameworks are applied to a variety of real-world networks to identify their corresponding MCRs. Furthermore, we explore how the demand magnitude as well as the demand pattern will affect their MCRs.

Table 3 presents the MCRs for 11 networks by solving the CP problem. In particular, the network topology, demand, and link performance functions of the networks can be found in Transportation Networks for Research Core Team (2016). As we can see, the MCR varies from network to network, ranging from 14.03% to 56.56%. However, except for three networks (Barcelona, Terrassa, and Winnipeg), the MCRs are all below 23%, suggesting that it is likely to achieve the SO in real-world networks by controlling only a small portion of AVs. In Sharon et al. (2018), the authors suggested that a larger network may require a greater fraction of CAVs to achieve SO as the number of paths grow. However, the comparison of the MCRs in Anaheim, Berlin-Friedrichshain, and Berlin-Mitte-Prenzlauerberg-Friedrichshain-Center networks in Table 3 suggests otherwise. There seems no distinct pattern for the relationship between the MCR and the size of the network.

Table 3: MCRs of various real-world networks

Network	# Zones	# Nodes	# Links	MCR (%)
Anaheim	38	416	914	20.52
Barcelona	110	1020	2522	35.96
Berlin-Friedrichshain (BF)	23	224	523	22.76
Berlin-Mitte-Center (BMC)	36	398	871	18.13
Berlin-Mitte-Prenzlauerberg-Friedrichshain-Center (BMPFC)	98	975	2184	14.03
Berlin-Prenzlauerberg-Center (BPC)	38	352	749	18.92
Berlin-Tiergarten (BT)	26	361	766	18.04
Eastern-Massachusetts (EM)	74	74	258	19.72
Sioux Falls (SF)	24	24	76	14.11
Terrassa	55	1609	3264	56.56
Winnipeg	147	1052	2836	41.78

4.1 Impact of demand magnitude

In this subsection, we explore the impact of demand magnitude on the MCRs corresponding to different networks. In particular, Fig. 7 shows the MCRs under various demand magnitudes. Specifically, the x-axis value "change of demand magnitude" indicates the percentage by which all the OD demands are reduced or increased. As observed, increasing the demand magnitude can result in increasing MCR for most of the tested networks, which is consistent with Proposition 1. However, for some tested networks, such as Sioux Falls and Terrassa, such a tendency does not hold. Instead, the increase of demand magnitude may decrease the MCR. The reason may be similar to the one discussed in Section 3.3. More specifically, the increase of demand magnitude may lead to a significant change of the shortest path set in these networks.

4.2 Impact of demand pattern

In addition to the demand magnitude, the demand pattern may also affect the MCR. To explore such an impact, we first define a $n \times n$ matrix $Q^{\xi} = \xi Q^C + (1-\xi)Q^S$, where n indicates the number of OD zones; $\xi \in [0,1]$; and Q^C and Q^S are complete and star networks, respectively. More specifically,

$$Q^C = \begin{bmatrix} 0 & \frac{1}{n-1} & \dots & \frac{1}{n-1} \\ \frac{1}{n-1} & 0 & \dots & \frac{1}{n-1} \\ \vdots & \vdots & \ddots & \vdots \\ \frac{1}{n-1} & \frac{1}{n-1} & \dots & 0 \end{bmatrix} \quad Q^S = \begin{bmatrix} 0 & \frac{1}{n-1} & \dots & \frac{1}{n-1} \\ 1 & 0 & \dots & 0 \\ \vdots & \vdots & \ddots & \vdots \\ 1 & 0 & \dots & 0 \end{bmatrix}$$

Therefore, Q^ξ is a convex combination of Q^C and Q^S. Denote $\hat{d}_i$ as the total demand from origin i. That is, $\hat{d}_i = \sum_{w:o(w)=i} \bar{d}_w$, where $o(w)$ indicates the origin of OD pair w. We then consider a class of demand patterns specified by the following $n \times n$ matrix $\boldsymbol{D}^\xi$:

$$\boldsymbol{D}^\xi = \begin{bmatrix} \hat{d}_1 & 0 & \dots & 0 \\ 0 & \hat{d}_2 & \dots & 0 \\ \vdots & \vdots & \ddots & \vdots \\ 0 & 0 & \dots & \hat{d}_n \end{bmatrix} Q^\xi$$

Specifically, D_{ij}^ξ denotes the travel demand from OD zone i to zone j. As we can see, when $\xi = 1$, all destinations have the same attraction for all origins, i.e., $D_{ij}^\xi = \frac{\hat{d}_i}{n-1}, \forall i, j, i \neq j$. When $\xi = 0$, travel demand from the center zone or the first origin, i.e., zone 1, will be equally distributed to all destinations $j \neq 1$; while demands from other origins $i \neq 1$ will all be attracted to zone 1. Therefore, changing the value of ξ, we can obtain different demand patterns.

Fig. 8 plots the MCRs corresponding to various demand patterns. As we can observe, when ξ increases from 0 to 1, the MCRs for most of the networks are shown to decrease. Nevertheless, there seems to be no clear tendency for Anaheim and BPC networks. It is worth highlighting that, as we have tested in some networks, the choice of the center zone in the star network may also have a great impact on the changing tendency of MCRs, but the specific effect may vary from one network to another.

5 Joint Control and Pricing

5.1 Motivations

The discussions in previous sections demonstrate that AVs can be utilized as mobile actuators for managing network traffic. However, such a control scheme may require a widespread adoption of the AV technology, e.g., 56.56% for the Terrassa network, which is still a distant reality. More importantly, as AVs can be privately owned, not every AV will be a CAV, i.e., willing to be controlled. On the other hand, congestion pricing has been widely recognized to be an efficient instrument for incentivizing travel behavior changes, but it is often criticized for, among others, increasing the financial burden of the public. In this section, we explore combining market-based and technology-based instruments to overcome their respective weaknesses. Specifically, the introduction of congestion pricing may distinctively decrease the control ratio required for CAVs, while controlling a portion of vehicles can largely reduce the tolling burden on travelers. We show the synergy of these two instruments yields remarkable results in achieving SO in transportation networks.

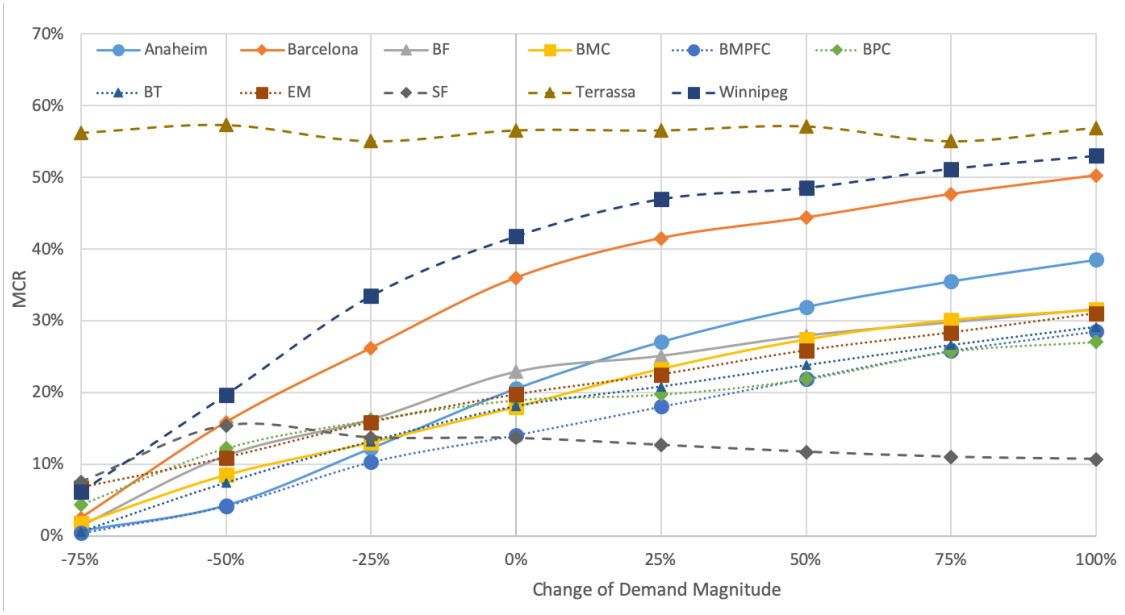

Figure 7: MCRs corresponding to various demand magnitudes

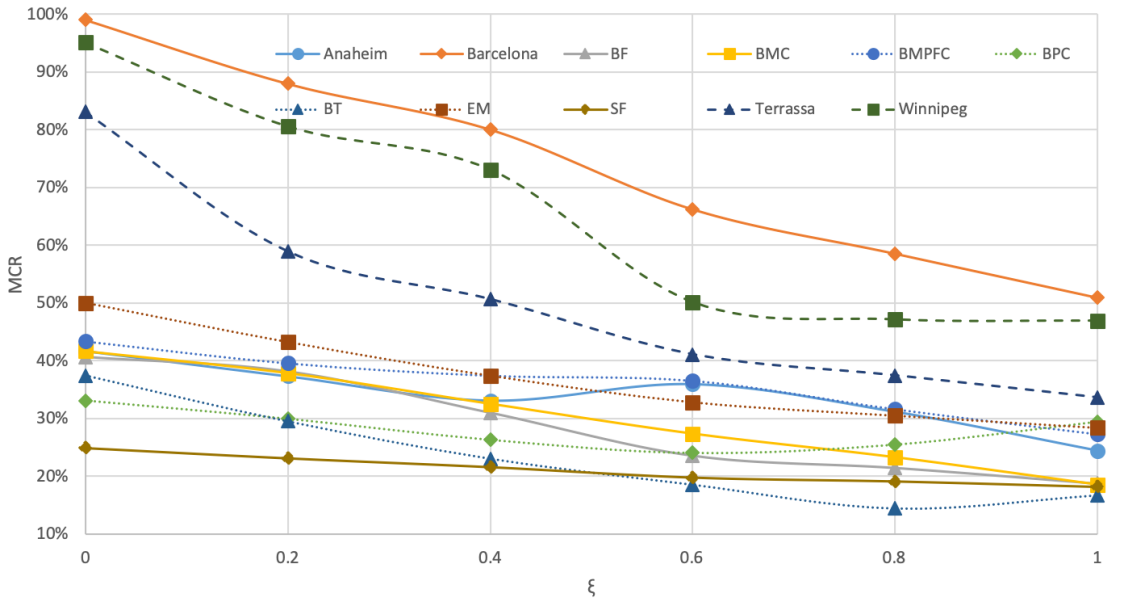

Figure 8: MCRs corresponding to various demand patterns

Among various congestion pricing schemes, we select the path-based pricing (Zangui et al., 2015) primarily because conceptually it matches well with the path controlling of AVs, and the level of connectivity will soon be ready to support the differentiation of paths traveled by different vehicles. It is worth highlighting that, as the routing of CAVs is controlled, only SVs will be imposed with the path-differentiated toll. The objectives are two-fold: we require both the proportion of CAVs and the revenue generated from the pricing scheme to be minimized. The above two objectives generally conflict with each other; therefore, we formulate the problem into a bi-objective optimization problem and generate its corresponding Pareto frontier below.

5.2 Model formulation

Before presenting the model, we first define the set of feasible path flows replicating SO for notational brevity. We say $\boldsymbol{f} \in \mathcal{F}$ if the following constraints are satisfied:

$$v_a^U = \sum_{w \in W} \sum_{r \in \bar{R}_w} f_r^U \delta_{a,r} \qquad \forall a \in A \tag{24}$$

$$\sum_{r \in \bar{R}_w} f_r^U = d_w^U \qquad \forall w \in W \tag{25}$$

$$f_r^U \geq 0 \qquad \forall r \in \bar{R}_w, w \in W \tag{26}$$

$$v_a^C = \sum_{w \in W} \sum_{r \in \bar{R}_w} f_r^C \delta_{a,r} \qquad \forall a \in A \tag{27}$$

$$\sum_{r \in \bar{R}_w} f_r^C = d_w^C \qquad \forall w \in W \tag{28}$$

$$f_r^C \geq 0 \qquad \forall r \in \bar{R}_w, w \in W \tag{29}$$

$$v_a^U + v_a^C = \bar{v}_a \qquad \forall a \in A \tag{30}$$

$$d_w^U + d_w^C = \bar{d}_w \qquad \forall w \in W \tag{31}$$

Constraints (24)-(31) are similar to constraints (1)-(8) except that f_r^U is defined on MMTT paths here; as the path-based pricing is implemented to replicate SO, every utilized path must be with the MMTTs with the presence of tolling scheme. Thus, we can write the joint control and pricing (JCP) problem as follows:

$$\min_{\boldsymbol{f^U}, \boldsymbol{f^C}, \boldsymbol{d^U}, \boldsymbol{d^C}, \boldsymbol{v^U}, \boldsymbol{v^C}, \boldsymbol{\gamma}, \boldsymbol{\mu}, \boldsymbol{X}} \left(\sum_{w \in W} \sum_{r \in \bar{R}_w} f_r^U \gamma_r, \sum_{w \in W} d_w^C \right)$$

$$\text{s.t.} \quad f_r^U \leq \bar{d}_w X_r \qquad \forall r \in \bar{R}_w, w \in W \tag{32}$$

$$\bar{t}_r + \gamma_r - \mu_w \leq K(1 - X_r) \qquad \forall r \in \bar{R}_w, w \in W \tag{33}$$

$$\bar{t}_r + \gamma_r - \mu_w \geq 0 \qquad \forall r \in \bar{R}_w, w \in W \tag{34}$$

$$\gamma_r \geq 0 \qquad \forall r \in \bar{R}_w, w \in W \tag{35}$$

$$X_r \in \{0, 1\} \qquad \forall r \in \bar{R}_w, w \in W \tag{36}$$

$$(\boldsymbol{f^U}, \boldsymbol{f^C}, \boldsymbol{d^U}, \boldsymbol{d^C}, \boldsymbol{v^U}, \boldsymbol{v^C}) \in \mathcal{F}$$

In the above model, $\bar{t}_r = \sum_{a \in A} t_a(\bar{v}_a)\delta_{a,r}$ is the SO travel time for path $r \in \bar{R}_w, w \in W$, γ_r is the associated path toll amount, and μ_w is the minimum generalized travel cost between OD pair $w \in W$. The objective function contains two components: the first component is the total revenue, i.e., $\sum_{w \in W} \sum_{r \in \bar{R}_w} f_r^U \gamma_r$, and the second is the total number of CAVs, i.e., $\sum_{w \in W} d_w^C$. We introduce a binary variable X_r to identify usable paths for SVs, where $X_r = 1$ implies the SV can use this path and $X_r = 0$ otherwise. Constraints (32) and (33) imply SV drivers will only choose the paths with the minimum generalized travel cost, i.e., $\bar{t}_r + \gamma_r$, where K is a sufficiently large number. Here we note that such constraints are only necessary for paths in $\bar{R}_w$ because we can always set a large toll amount to prevent SVs from using other paths. Constraint (34) states the minimum nature of μ_w. Constraint (35) states that the path toll must be non-negative, and Constraint (36) suggests the binary nature of X_r.

As formulated, JCP is a bi-objective mixed-integer program with nonlinear terms in the objective function, i.e., $\sum_{w\in W}\sum_{r\in\bar{R}_w} f_r^U \gamma_r$. Such a problem is thus extremely difficult to solve optimally. In conventional SO decentralization, $\sum_{w\in W}\sum_{r\in\bar{R}_w} f_r^U \gamma_r$ can often be equivalently transformed into a linear term $\sum_{w\in W} \bar{d}_w \mu_w$ (e.g., Zangui et al., 2015), but such transformation is infeasible in JCP because the demand related to SVs is d_w^C, which is itself a variable. Fortunately, we can still utilize the following property of path-differentiated tolls to linearize the above formulation. Consider the set of utilized paths between OD pair w by SVs, say $r_1, r_2, ..., r_n$, where $\bar{t}_{r_1} \geq \bar{t}_{r_2} \geq ... \geq \bar{t}_{r_n}$; we call r_1 the "longest utilized path". By Constraint (33), we know these paths share the same generalized travel costs, denoted by μ_w. Apparently, for any given SV path flows, setting $\gamma_{r_i} = \bar{t}_{r_1} - \bar{t}_{r_i}, \forall i \in 1, 2, ..., n$ leads to the minimum revenue for this OD pair, and in such a case the longest utilized path is toll-free. Such a phenomenon is also highlighted in Zangui et al. (2015). Therefore, the path toll on any utilized path is determined once the longest utilized path is known, and with this property we are able to linearize the objective function of JCP.

We introduce an additional binary variable Y_r to represent the selection of the longest utilized path for OD pair $w \in W$, where $Y_r = 1$ represents that path r is chosen as the longest utilized path in w and $Y_r = 0$ otherwise; apparently we have $\sum_{r\in\bar{R}_w} Y_r = 1$. Then we can rewrite γ_r as $\sum_{r'\in\bar{R}_w} Y_{r'} \max(0, \bar{t}_{r'} - \bar{t}_r)$, suggesting that the path toll is $\max(0, \bar{t}_{r'} - \bar{t}_r)$ if path r' is chosen as the longest utilized path. Then we have $f_r^U \gamma_r = \sum_{r'\in\bar{R}_w} f_r^U Y_{r'} \max(0, \bar{t}_{r'} - \bar{t}_r)$. By introducing another auxiliary variable $Z_{r,r'} = f_r^U Y_{r'}$, we can then reformulate JCP as follows:

$$\min_{\boldsymbol{f^U}, \boldsymbol{f^C}, \boldsymbol{d^U}, \boldsymbol{d^C}, \boldsymbol{v^U}, \boldsymbol{v^C}, \boldsymbol{Y}, \boldsymbol{Z}} \left(\sum_{w\in W} \sum_{r\in\bar{R}_w} \sum_{r'\in\bar{R}_w} Z_{r,r'} \max(0, \bar{t}_{r'} - \bar{t}_r), \sum_{w\in W} d_w^C \right)$$

$$\text{s.t.} \quad f_r^U \leq \bar{d}_w \sum_{r'\in\bar{R}_w : \bar{t}_{r'} \geq \bar{t}_r} Y_{r'} \qquad \forall r \in \bar{R}_w, w \in W \qquad (37)$$

$$\sum_{r\in\bar{R}_w} Y_r = 1 \qquad \forall w \in W \qquad (38)$$

$$f_r^U - \bar{d}_w(1 - Y_{r'}) \leq Z_{r,r'} \leq \bar{d}_w Y_{r'} \qquad \forall r, r' \in \bar{R}_w, w \in W \qquad (39)$$

$$0 \leq Z_{r,r'} \leq f_r^U \qquad \forall r, r' \in \bar{R}_w, w \in W \qquad (40)$$

$$Y_r \in \{0, 1\} \qquad \forall r \in \bar{R}_w, w \in W \qquad (41)$$

$$(\boldsymbol{f^U}, \boldsymbol{f^C}, \boldsymbol{d^U}, \boldsymbol{d^C}, \boldsymbol{v^U}, \boldsymbol{v^C}) \in \mathcal{F}$$

In the reformulated JCP, the objective function is transformed into equivalent linear terms. Constraint (37) states that only paths with shorter or equal travel time compared to the longest utilized path can support SV flows, because $\sum_{r'\in\bar{R}_w : \bar{t}_{r'} \geq \bar{t}_r} Y_{r'} = 0$ if the travel time of path r is longer than that of the selected longest utilized one. Constraint (38) requires that only one path is selected as the longest utilized path for each OD pair. Constraints (39) and (40) together restrict that $Z_{r,r'} = 0$ if $Y_{r'} = 0$, and $Z_{r,r'} = f_r^U$ if $Y_{r'} = 1$, i.e., $Z_{r,r'} = f_r^U Y_{r'}$; Constraint (41) states the binary nature of Y_r. Compared to the original JCP formulation, the reformulated one neutralizes the nonlinear terms, then it becomes a bi-objective mixed-integer linear program (B-MILP). The next subsection will introduce the solution procedure to find the Pareto frontier of JCP.

5.3 Solution procedure

A solution is said to be on the Pareto frontier of JCP if there is no other feasible solution that can dominate both the total revenue and the control ratio. Specifically, there are two extreme points on the Pareto frontier: one is the "zero revenue" point, which is obtained by solving the JCP problem with zero revenue, and where the corresponding control ratio is dubbed "zero-revenue control ratio" or ZRCR; and the other is the "zero control" point, which is obtained by solving the JCR problem without the presence of CAVs or the minimum-revenue path-differentiated toll problem proposed by Zangui et al. (2015), and the corresponding revenue is dubbed "zero-control-ratio revenue" or ZCRR. By definition, a straightforward way of generating the Pareto frontier is to put the second objective, i.e., the total number of CAVs, into the constraint, and explore the whole frontier by traversing the interval of feasible boundaries on the number of CAVs. Mathematically, we can define the following single-objective optimization problem, denoted by JCP($\bar{D}$), as:

$$
\begin{aligned}
&\min_{\boldsymbol{f^U}, \boldsymbol{f^C}, \boldsymbol{d^U}, \boldsymbol{d^C}, \boldsymbol{v^U}, \boldsymbol{v^C}, \boldsymbol{Y}, \boldsymbol{Z}} \sum_{w \in W} \sum_{r \in \bar{R}_w} \sum_{r' \in \bar{R}_w} Z_{r,r'} \max(0, \bar{t}_{r'} - \bar{t}_r) \\
&\text{s.t.} \quad (37) - (41) \\
&\sum_{w \in W} d_w^C \leq \bar{D} \qquad (42) \\
&(\boldsymbol{f^U}, \boldsymbol{f^C}, \boldsymbol{d^U}, \boldsymbol{d^C}, \boldsymbol{v^U}, \boldsymbol{v^C}) \in \mathcal{F}
\end{aligned}
$$

We observe that JCP($\bar{D}$) is a standard mixed-integer linear program (MILP), which can be solved by well-established commercial software (e.g., CPLEX). The feasible choice of $\bar{D}$ is $[0, D_{ZR}]$, where D_{ZR} is the demand associated with ZRCR. By choosing a set of uniformly distributed values in $[0, D_{ZR}]$ and solving JCP($\bar{D}$) upon these values we can acquire a rough layout of the Pareto frontier.

Below we present a method for calculating the D_{ZR}, which should not be confused with the solution to the problem of CP as defined in Section 2.1. The presence of path-based pricing may help further reduce the number of CAVs required to achieve SO without collecting any revenue. In other words, we can utilize path pricing to obviate the use of some paths for the minimization of the control ratio. The JCP problem with zero revenue (JCP-ZR) is mathematically formulated as follows:

$$
\begin{aligned}
&\min_{\boldsymbol{f^U}, \boldsymbol{f^C}, \boldsymbol{d^U}, \boldsymbol{d^C}, \boldsymbol{v^U}, \boldsymbol{v^C}, \boldsymbol{Y}} \sum_{w \in W} d_w^C \\
&\text{s.t.} \quad f_r^U \leq \bar{d}_w \sum_{r' \in \bar{R}_w : \bar{t}_{r'} = \bar{t}_r} Y_{r'} && \forall r \in \bar{R}_w, w \in W && (43) \\
&\sum_{r \in \bar{R}_w} Y_r = 1 && \forall w \in W && (44) \\
&Y_r \in \{0, 1\} && \forall r \in \bar{R}_w, w \in W && (45) \\
&(\boldsymbol{f^U}, \boldsymbol{f^C}, \boldsymbol{d^U}, \boldsymbol{d^C}, \boldsymbol{v^U}, \boldsymbol{v^C}) \in \mathcal{F}
\end{aligned}
$$

In the above model, the objective is to minimize the number of CAVs, and Y_r is the binary variable to indicate the chosen paths to be toll-free. Constraint (43) suggests that only paths

with $Y_r = 1$ (or with the same travel time as a path such that $Y_r = 1$) are allowed to support positive SV flows; other paths are set with prohibitively large tolls to prevent SV drivers from using them. As a result, no tolling path could attract SV flows, and thus no revenue is collected. Constraint (44) indicates that for any OD pair, only paths with the same travel time are allowed to be utilized by SVs. Constraint (45) states the binary nature of Y_r. JCP-ZR is also an MILP, which could be effectively solved by commercial software. The optimal objective function value of JCP-ZR is used as the upper bound of feasible interval for Pareto frontier, i.e., D_{ZR}.

Recall that in the absence of pricing, there exist some specific networks requiring 100% vehicle control to achieve SO. Interestingly, with the introduction of path-based pricing, an upper bound for ZRCR exists, which is strictly less than one. The details are given as follows:

Proposition 4. *For a given network and OD demand, the ZRCR is upper bounded by* $\frac{\sum_w \bar{d}_w(1-\frac{1}{n_w})}{\sum_w \bar{d}_w}$, *where* n_w *is the number of MMTT paths between OD pair* w.

Proof. From JCP-ZR, we see that the essence of a zero-revenue pricing and control problem is to select one path (or a set of paths with the same travel time) for each OD pair as the non-controlled path(s). For any given SO path flow pattern $\boldsymbol{f}$, we can always select the path with the largest flow for each OD pair as the non-controlled path by charging sufficiently high pricing on other paths. For this OD pair, the number of CAVs is no more than $\bar{d}_w(1-\frac{1}{n_w})$, thus the total control ratio is upper bounded by $\frac{\sum_w \bar{d}_w(1-\frac{1}{n_w})}{\sum_w \bar{d}_w}$. Proof completes. □

The above proposition offers a promising prospect on the minimum control ratio, because many realistic networks are filled with OD pairs with only one MMTT path. For example, as shown by Zangui et al. (2015), the number of OD pairs with a unique MMTT path is approximately 62% of the total for Sioux Falls and 81% for Anaheim. Since $n_w = 1$ for these OD pairs, we have $\bar{d}_w(1-\frac{1}{n_w}) = 0$, suggesting that they contribute no CAVs to the whole required number, and naturally the overall control ratio could be significantly lowered. Such an observation is further confirmed by the numerical examples in the following subsection.

Lastly, we present the detailed procedure for obtaining the layout of Pareto frontier for JCP.

- **Step 1**. Solve JCP-ZR and obtain the optimal objective function value D_{ZR}; solve the JCP(0) problem and obtain the optimal objective function value R_0, i.e., ZCRR.
- **Step 2**. Uniformly sample n points in interval $[0, D_{ZR}]$, i.e., $\bar{D}_1, \bar{D}_2, ..., \bar{D}_n$, and solve JCP($\bar{D}_i$), $i \in \{1, 2, ..., n\}$ accordingly. The corresponding objective function values are $R_i, i \in \{1, 2, ..., n\}$.
- **Step 3**. Connect the points $(0, R_0), (\bar{D}_1, R_1), (\bar{D}_2, R_2), ..., (\bar{D}_n, R_n), (D_{ZR}, 0)$. The curve is the approximated Pareto frontier.

5.4 Numerical Example

Applying the above procedure with $n = 8$, we obtain the Pareto frontiers of JCP on Anaheim and Barcelona networks, shown in Fig. 9. Meanwhile, Table 4 specifies ZRCRs, MCRs, the decrements of the former compared with the latter, the proportion of OD pairs with a unique path, and the upper bound of ZRCRs provided by Proposition 4, for all real-world networks considered in this paper. Some observations can be drawn:

- Based on Fig. 9, as the allowable control ratio increases, the collected revenue will decrease. Particularly, when the control ratio is 0, i.e., there exists no CAV, the revenue, i.e., ZCRR, is in fact the revenue collected by the minimum-revenue path-differentiated pricing scheme proposed by Zangui et al. (2015). Specifically, the ZCRRs are 2180.73 and 667.48 minutes for the two networks, respectively.

- It is possible to achieve SO by controlling a proportion of CAVs much lower than MCR with a pricing scheme that generates much less revenue than the ZCRR. For example, in the Barcelona network, the SO can be achieved by controlling only 0.175% vehicles and collecting a total revenue equivalent to approximately 29 minutes (see Fig. 9(b)), which represents a 99.51% reduction in control ratio compared to the MCR, and a 95.63% reduction in toll revenue compared to the ZCRR. This phenomenon suggests that combining congestion pricing and path controlling schemes could generate substantial synergistic effect.

- The ratios between the ZCRR and the SO travel time are calculated to be 0.16% and 0.05% for Anaheim and Barcelona networks, respectively. Together with their ZRCRs shown in Table 4, it seems to imply that the tiny ZRCR for Anaheim and Barcelona networks is the result of the tiny ZCRR. That is, the smaller the ZCRR is, the smaller ZRCR will be. It seems plausible as, to some extent, the former suggests that a smaller number of vehicles is required to be controlled. However, this may not be necessarily true (see Appendix B).

- One interesting finding from Table 4 is that the ZRCRs for the networks are all much lower than their MCRs, and the decrements are quite significant (e.g., 96.45% and 99.12% for Anaheim and Barcelona, respectively). That is, by designing an appropriate path-differentiated pricing scheme, the SO can be achieved with zero revenue and a level of CAVs that is much smaller than the MCR. Since only SVs are charged for the toll, imposing a sufficiently high toll on particular paths is equivalent to converting these paths into CAV-only paths, because no SV would choose to use them. Therefore, regulating the routing strategy of SVs may actually require collecting no toll. Furthermore, as shown in Table 4, except for Terrassa, all the tested networks posses a large number of OD pairs (more than 50%) with a unique MMTT path, such as Anaheim (80.87%) and BMPFC (90.75%). As the ZRCR for these OD pairs must be 0, the ZRCR for these networks can be very small.

- Table 4 indicates that the upper bound of ZRCR provided by Proposition 4 could be much smaller than the MCRs if the networks are with a large number of OD pairs with a unique MMTT path, such as Anaheim (80.87%) and BMPFC (90.75%). However, for the networks with a small number of OD pairs with a unique MMTT path, such as Terrassa (22.26%), their upper bounds could be even higher than their MCRs.

6 Conclusion

Envisioning that automated vehicles may act as mobile actuators to regulate traffic flow across road networks, this paper has proposed a path controlling scheme to achieve the system optimum by controlling the routing of a portion of automated vehicles. Finding the minimum control ratio of the scheme is delineated by a linear program, which can be solved efficiently by commercial solvers. Mathematical proof and numerical examples based on real-world transportation networks are offered to characterize the minimum control ratio. A few findings

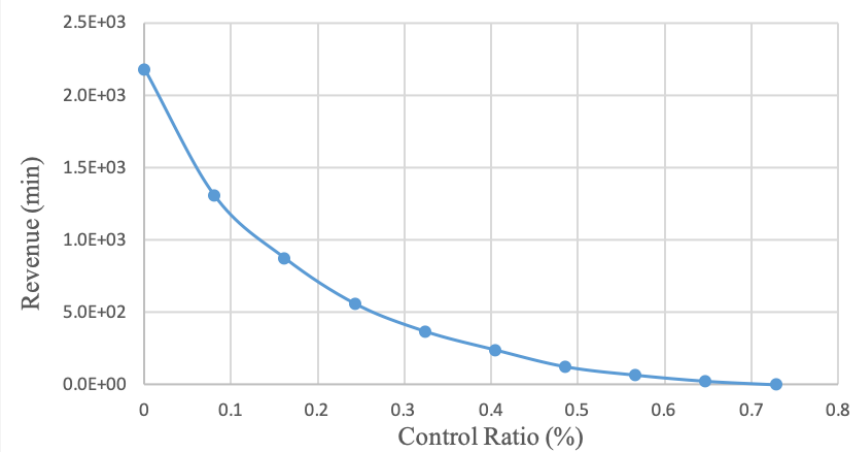

(a)

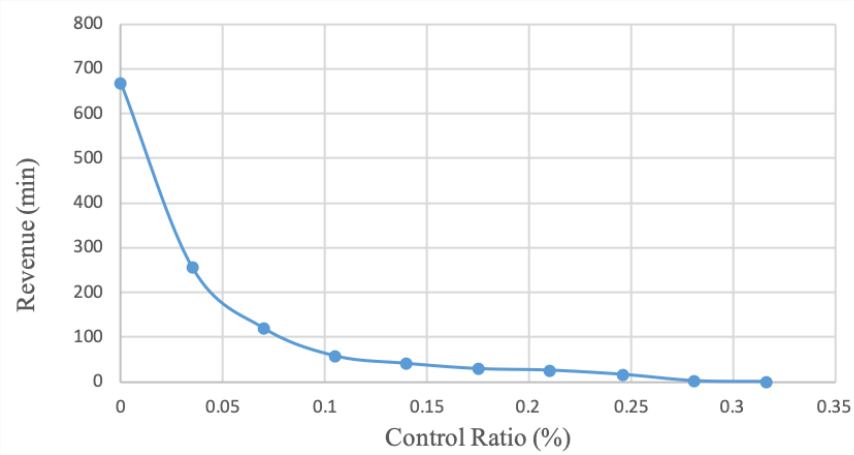

(b)

Figure 9: Pareto frontiers of JCP on (a) Anaheim, and (b) Barcelona networks

Table 4: Results for real-world networks

Network	ZRCR (%)	MCR (%)	Decrement (%)	OD Pairs with Unique Path (%)	Upper Bound of ZRCR (%)
Anaheim	0.73	20.52	96.45	80.87	13.27
Barcelona	0.32	35.96	99.12	63.14	20.79
BF	0.92	22.76	95.95	78.26	14.03
BMC	0.35	18.13	98.10	85.87	14.15
BMPFC	0.06	14.03	99.58	90.75	4.37
BPC	0.30	18.92	98.42	81.37	11.07
BT	0.41	18.04	97.75	83.23	11.80
EM	0.48	19.72	97.55	75.83	16.15
SF	0.70	14.11	95.07	61.93	20.94
Terrassa	23.64	56.56	58.21	22.26	73.07
Winnipeg	0.60	41.78	98.57	54.61	31.12

are worth highlighting here. We show that the minimum control ratio varies from 0 to 1,

depending on the network topology and demand pattern. In our tested networks, it ranges between 14.03% and 56.56%, but is below 23% for the majority of them. Given that the required minimum control ratio can be high (e.g., 35.96%, 41.78%, and 56.56% for Barcelona, Winnipeg, and Terrassa networks, respectively), we have further proposed a joint control and pricing scheme that combines the path controlling of cooperative automated vehicles and the path-based pricing of conventional vehicles or uncontrolled automated vehicles. The design of the scheme is formulated as a mixed-integer linear program. Numerical examples demonstrate the substantial synergistic effect of the joint scheme on reducing the minimum control ratio and the financial burden on travelers. For example, the joint scheme can reduce the the minimum control ratios by approximately 96% and 99% for Anaheim and Barcelona networks, respectively, without collecting any tolling revenue.

Acknowledgements

The work described in this paper was partly supported by research grants from the National Science Foundation (CNS-1837245; CMMI-1854684) and National Science Foundation of China (51622807). We also would like to thank Lloyd's Register Foundation (LRF) for the support. LRF helps to protect life and property by supporting engineering-related education, public engagement and the application of research.

Appendix A

To avoid the enumeration of the sets of shortest paths and MMTT paths, we develop a column generation algorithm to solve the CP problem. Specifically, we define the subsets of the shortest paths and MMTT paths as $\hat{P}_w$ and $\bar{P}_w$, respectively, and introduce a restricted CP (RCP) problem, as shown below:

$$\min_{f^U, f^C, d^U, d^C, v^U, v^C} \sum_{w \in W} d_w^C$$

$$\text{s.t.} \quad v_a^U = \sum_{w \in W} \sum_{r \in \hat{P}_w} f_r^U \delta_{a,r} \qquad \forall a \in A \tag{46}$$

$$\sum_{r \in \hat{P}_w} f_r^U = d_w^U \qquad \forall w \in W \tag{47}$$

$$f_r^U \geq 0 \qquad \forall r \in \hat{P}_w, w \in W \tag{48}$$

$$v_a^C = \sum_{w \in W} \sum_{r \in \bar{P}_w} f_r^C \delta_{a,r} \qquad \forall a \in A \tag{49}$$

$$\sum_{r \in \bar{P}_w} f_r^C = d_w^C \qquad \forall w \in W \tag{50}$$

$$f_r^C \geq 0 \qquad \forall r \in \bar{P}_w, w \in W \tag{51}$$

$$v_a^U + v_a^C = \bar{v}_a \qquad \forall a \in A \tag{52}$$

$$d_w^U + d_w^C = \bar{d}_w \qquad \forall w \in W \tag{53}$$

The Lagrangian of RCP is thus given by

$$
\begin{aligned}
L = & \sum_{w\in W} d_w^C - \sum_{a\in A} \lambda_a^U \left(v_a^U - \sum_{w\in W} \sum_{r\in \hat{P}_w} f_r^U \delta_{a,r} \right) - \sum_{w\in W} \hat{\rho}_w \left(\sum_{r\in \hat{P}_w} f_r^U - d_w^U \right) \\
& - \sum_{a\in A} \lambda_a^C \left(v_a^C - \sum_{w\in W} \sum_{r\in \bar{P}_w} f_r^C \delta_{a,r} \right) - \sum_{w\in W} \bar{\rho}_w \left(\sum_{r\in \bar{P}_w} f_r^C - d_w^C \right) - \sum_{a\in A} \alpha_a \left(v_a^U + v_a^C - \bar{v}_a \right) \\
& - \sum_{w\in W} \beta_w \left(d_w^U + d_w^C - \bar{d}_w \right) \\
= & \sum_{w\in W} \sum_{r\in \hat{P}_w} \left(\sum_{a\in A} \lambda_a^U \delta_{a,r} - \hat{\rho}_w \right) f_r^U + \sum_{w\in W} \sum_{r\in \bar{P}_w} \left(\sum_{a\in A} \lambda_a^C \delta_{a,r} - \bar{\rho}_w \right) f_r^C + \sum_{w\in W} d_w^C - \sum_{a\in A} \lambda_a^U v_a^U \\
& + \sum_{w\in W} \hat{\rho}_w d_w^U - \sum_{a\in A} \lambda_a^C v_a^C + \sum_{w\in W} \bar{\rho}_w d_w^C - \sum_{a\in A} \alpha_a \left(v_a^U + v_a^C - \bar{v}_a \right) - \sum_{w\in W} \beta_w \left(d_w^U + d_w^C - \bar{d}_w \right)
\end{aligned}
$$

where $\boldsymbol{\lambda^U, \hat{\rho}, \lambda^C, \bar{\rho}, \alpha_a, \beta_w}$ are the multipliers of constraints (46), (47), (49), (50), (52), and (53), respectively.

According to the above Lagrangian, the reduced cost of any path $r \in \hat{R}_w$ is $\sum_{a\in A} \lambda_a^U \delta_{a,r} - \hat{\rho}_w$, and it must be no less than 0 for any path $r \in \hat{R}_w \setminus \hat{P}_w$ under optimality. Therefore, finding a new shortest path for an OD pair $w \in W$ that might improve the objective value is to solve the following shortest path finding (SP) problem:

$$
\begin{aligned}
& \min_{\hat{\boldsymbol{y}}^w} \sum_{a\in A} \lambda_a^U \hat{y}_a^w \\
& \text{s.t.} \quad \Delta \hat{\boldsymbol{y}}^w = \boldsymbol{E^w} && \forall w \in W \\
& \sum_{a\in A} t_a(\bar{v}_a) \hat{y}_a^w = \hat{c}^w && \forall w \in W \\
& \hat{y}_a^w \in \{0,1\} && \forall a \in A
\end{aligned}
$$

where $\hat{y}_a^w$ is a binary variable, which is equal to 1 if link a is utilized and 0 otherwise; $\hat{c}^w$ represents the shortest travel time between OD pair w, which can be predetermined given the SO flow distribution $\bar{v}$; Δ is the node-link incidence matrix associated with the network and E^w is the vector with a length of $|N|$. The vector consists of two-nonzero components: one has a value of 1 in the component corresponding to the origin of w, and the other has a value of -1 in the component corresponding to the destination of w. The first constraint ensures the flow conservation, and the second one is to guarantee that the selected path is a shortest path. For each OD pair $w \in W$, the optimal solution to SP can be used to construct a shortest path, i.e., $\hat{p}^w$, that could possibly improve the objective value of RCP.

Similarly, we have the following MMTT path finding (MMTTP) problem:

$$
\begin{aligned}
& \min_{\bar{\boldsymbol{y}}^w} \sum_{a\in A} \lambda_a^C \bar{y}_a^w \\
& \text{s.t.} \quad \Delta \bar{\boldsymbol{y}}^w = \boldsymbol{E^w} && \forall w \in W \\
& \sum_{a\in A} \bar{t}_a(\bar{v}_a) \bar{y}_a^w = \bar{c}^w && \forall w \in W
\end{aligned}
$$

$$\bar{y}_a^w \in \{0,1\} \qquad \forall a \in A$$

where $\bar{y}_a^w$ is a binary variable, which is equal to 1 if link a is utilized and 0 otherwise; $\bar{c}^w$ represents the MMTT between OD pair w, which can be easily calculated with the SO flow distribution $\bar{v}$; For each OD pair $w \in W$, the optimal solution to MMTTP can be used to construct a MMTT path, i.e., $\bar{p}^w$, that could possibly improve the objective value of RCP.

The column generation algorithm is presented as follows:

- **Step 1**. Solve the SO flow assignment via the path column generation process; obtain $\bar{v}$, $\bar{c}$, and the corresponding subset of MMTT paths, i.e., $\bar{P}$. Note that with $\bar{P}$ as an initial marginal shortest path subset, the feasibility of RCP can always be guaranteed.
- **Step 2**. Solve SP problem with $\lambda_a^U = t_a(\bar{v}_a), \forall a \in A$ for each OD pair; obtain $\hat{c}^w$, and construct $\hat{P}^w = \{\hat{p}^w\}$ for all $w \in W$.
- **Step 3**. Solve RCP upon $\hat{P}^w$ and $\bar{P}^w$, and obtain $\boldsymbol{d^C}$ and the multipliers $\boldsymbol{\lambda^U, \hat{\rho}, \lambda^C}$,and $\bar{\boldsymbol{\rho}}$.
- **Step 4**. For each OD pair $w \in W$, solve SP and MMTTP upon $\boldsymbol{\lambda^U}$ and $\boldsymbol{\lambda^C}$; obtain paths $\hat{p}^w$ and $\bar{p}^w$. For $w \in W$, if $\sum_{a \in A(\hat{p}^w)} \lambda_a^U \hat{y}_a^w < \hat{\rho}^w$, add $\hat{p}^w$ to $\hat{P}^w$; similarly, if $\sum_{a \in A(\bar{p}^w)} \lambda_a^C \bar{y}_a^w < \bar{\rho}^w$, add $\bar{p}^w$ to $\bar{P}^w$. However, if $\sum_{a \in A(\hat{p}^w)} \lambda_a^U \hat{y}_a^w \geq \hat{\rho}^w$ and $\sum_{a \in A(\bar{p}^w)} \lambda_a^C \bar{y}_a^w \geq \bar{\rho}^w$ for all OD pairs, stop and $\boldsymbol{d}^C$ is the optimal solution. $\sum_{w \in W} d_w^C$ is thus the minimum number of CAVs to achieve SO. Otherwise, go to **Step 3**.

Appendix B

This appendix illustrates that a small ZCRR does not necessarily imply a small ZRCR and vice versa.

Consider a parallel network as shown in Fig. 2. Assume there are two parallel links with associated link travel time functions as $t_1(x) = 1 + x$ and $t_2(x) = 1 + \delta + x$ where x is the link flow and $\delta > 0$ is a sufficiently small number. Given a total demand of d, the SO state is calculated as $\bar{x}_1 = \frac{d}{2} + \frac{\delta}{4}$ and $\bar{x}_2 = \frac{d}{2} - \frac{\delta}{4}$, and we have $t_1(\bar{x}_1) = 1 + \frac{d}{2} + \frac{\delta}{4}$, $t_2(\bar{x}_2) = 1 + \frac{d}{2} + \frac{3\delta}{4}$. To achieve SO, we only need to charge a toll on link 1 with the amount of $\frac{\delta}{2}$, generating a revenue of $\frac{\delta}{2}\bar{x}_1 = \frac{d\delta}{4} + \frac{\delta^2}{8} \approx 0$. On the other hand, the ZRCR is equal to $\bar{x}_2/d = \frac{1}{d}(\frac{d}{2} - \frac{\delta}{4}) \approx \frac{1}{2}$. Such an example shows that a network with almost zero ZCRR can still have a large ZRCR.

Then we show that a network with small ZRCR could result in a large ZCRR. Consider a parallel network with two links, where the associated link travel time functions are $t_1(x) = 1 + 100x$ and $t_2(x) = 100 + x$, and the total demand is given by $d = \frac{99}{200} + \delta$, where $\delta > 0$ is a sufficiently small number. The SO state is given by $\bar{x}_1 = \frac{99}{200} + \frac{1}{101}\delta$ and $\bar{x}_2 = \frac{100}{101}\delta$, and we have $t_1(\bar{x}_1) = \frac{101}{2} + \frac{100}{101}\delta$, $t_2(\bar{x}_2) = 100 + \frac{100}{101}\delta$. For ZCRR, we must charge a toll of $\frac{99}{2}$ on link 1, resulting in a revenue of $\frac{9801}{400} + \frac{99}{202}\delta$, but the ZRCR is $\bar{x}_2/d \approx \frac{20000}{9999}\delta \approx 0$. Thus, a network with high ZCRR could still have a negligible ZRCR.

References

Colini-Baldeschi, R., Cominetti, R., Mertikopoulos, P., and Scarsini, M. (2017). The asymptotic behavior of the price of anarchy. In *International Conference on Web and Internet Economics*, pages 133–145. Springer.

Colini-Baldeschi, R., Cominetti, R., and Scarsini, M. (2019). Price of anarchy for highly congested routing games in parallel networks. *Theory of Computing Systems*, 63(1):90–113.

Harker, P. T. (1988). Multiple equilibrium behaviors on networks. *Transportation science*, 22(1):39–46.

Hearn, D. W. and Ramana, M. V. (1998). Solving congestion toll pricing models. In *Equilibrium and advanced transportation modelling*, pages 109–124. Springer.

Jin, I. G., Avedisov, S. S., He, C. R., Qin, W. B., Sadeghpour, M., and Orosz, G. (2018). Experimental validation of connected automated vehicle design among human-driven vehicles. *Transportation research part C: emerging technologies*, 91:335–352.

Li, R., Liu, X., and Nie, Y. (2018). Managing partially automated network traffic flow: Efficiency vs. stability. *Transportation Research Part B: Methodological*, 114:300–324.

Sharon, G., Albert, M., Rambha, T., Boyles, S., and Stone, P. (2018). Traffic optimization for a mixture of self-interested and compliant agents. In *Thirty-Second AAAI Conference on Artificial Intelligence*.

Stern, R. E., Cui, S., Delle Monache, M. L., Bhadani, R., Bunting, M., Churchill, M., Hamilton, N., Pohlmann, H., Wu, F., Piccoli, B., et al. (2018). Dissipation of stop-and-go waves via control of autonomous vehicles: Field experiments. *Transportation Research Part C: Emerging Technologies*, 89:205–221.

Transportation Networks for Research Core Team (2016). Transportation networks for research. `https://github.com/bstabler/TransportationNetworks`. Accessed on July 13, 2018.

Wang, M. (2018). Infrastructure assisted adaptive driving to stabilise heterogeneous vehicle strings. *Transportation Research Part C: Emerging Technologies*, 91:276–295.

Wardrop, J. G. (1952). Some theoretical aspects of road traffic research. In *Inst Civil Engineers Proc London/UK/*.

Wu, C., Bayen, A. M., and Mehta, A. (2018). Stabilizing traffic with autonomous vehicles. In *2018 IEEE International Conference on Robotics and Automation (ICRA)*, pages 1–7. IEEE.

Wu, C., Kreidieh, A., Parvate, K., Vinitsky, E., and Bayen, A. M. (2017). Flow: Architecture and benchmarking for reinforcement learning in traffic control. *arXiv preprint arXiv:1710.05465*.

Yang, H., Han, D., and Lo, H. K. (2008). Efficiency of atomic splittable selfish routing with polynomial cost functions. *Networks and Spatial Economics*, 8(4):443–451.

Yang, H. and Wang, X. (2011). Managing network mobility with tradable credits. *Transportation Research Part B: Methodological*, 45(3):580–594.

Yang, H., Zhang, X., and Meng, Q. (2007). Stackelberg games and multiple equilibrium behaviors on networks. *Transportation Research Part B: Methodological*, 41(8):841–861.

Zangui, M., Aashtiani, H. Z., Lawphongpanich, S., and Yin, Y. (2015). Path-differentiated pricing in congestion mitigation. *Transportation Research Part B: Methodological*, 80:202–219.

Zangui, M., Yin, Y., Lawphongpanich, S., and Chen, S. (2013). Differentiated congestion pricing of urban transportation networks with vehicle-tracking technologies. *Transportation Research Part C*, 36:434–445.

Zhang, K. and Nie, Y. M. (2018). Mitigating the impact of selfish routing: An optimal-ratio control scheme (orcs) inspired by autonomous driving. *Transportation Research Part C: Emerging Technologies*, 87:75–90.

Zhang, X., Yang, H., and Huang, H.-J. (2008). Multiclass multicriteria mixed equilibrium on networks and uniform link tolls for system optimum. *European Journal of Operational Research*, 189(1):146–158.